BCAL Resolution Study using HDFast

G.M. Huber

Department of Physics, University of Regina, Regina, SK, S4S 0A2, Canada

(Dated: November 12, 2004)

The effects of finite energy and position resolution are investigated using HDFast, for photons detected in the BCAL. Depending on the reaction simulated, the obtained invariant mass resolution is between 15 and 45 MeV, which in all cases is better than the minimum resolution requirement of $\sigma(m_{\Sigma\gamma}) < m_{\pi^0}/2$. It is also found that the invariant mass resolution is significantly more sensitive to the BCAL position resolution in the azimuthal direction than in the longitudinal direction, and this might be an important consideration when optimizing the azimuthal readout segmentation of the BCAL.

I. INTRODUCTION

For its study of exotic hybrid mesons, the GlueX detector is intended to be a hermetic detector with good particle identification and momentum and angular resolution characteristics. These are necessary for the identification of the J^{PC} and decay modes of any exotic hybrid candidates via a partial wave analysis. One of the necessary criteria in the operation of the experiment is to know, on an event-by-event basis, whether kinematic completeness has been achieved.

The Barrel Calorimeter (BCAL) and Lead Glass Detector (LGD) together play an important role in the operation of the GlueX detector, as they are responsible for the detection of photons, through electromagnetic calorimetry. The BCAL subtends photon emission angles of approximately $11^o < \theta < 127^o$, while the LGD covers very forward angles, $\theta < 12.8^o$ [1]. Thus, while good acceptance for charged particles is very important, this study will restrict itself to the emission of photons. In this case, kinematic completeness comes down to knowing the number of missing π^0s per event. One way to investigate this is to simulate some common neutral decay modes of neutral mesons under various assumptions, and see whether the resulting invariant mass reconstruction is sufficiently good to exclude the emission of an additional π^0, i.e. $\sigma(m_{\Sigma\gamma}) < m_{\pi^0}/2$. The emphasis of this report is upon the effects of the finite position and energy resolution of the BCAL detector.

This note is an update to the 2001 BCAL resolution study by S. Teige [2].

II. RESOLUTION SMEARING

Energy Resolution

The energy resolution of an electromagnetic calorimeter is usually written as the square root over the quadratic sum of three terms

$$\frac{\sigma(E)}{E} = \frac{a}{\sqrt{E}} \oplus b \oplus \frac{c}{E}$$

The first term a is known as the stochastic term of the energy resolution, and is due to a number of factors, including sampling fluctuations and intrinsic shower fluctuations in the signal generating process. a can be reduced by improving light collection efficiency or production. The second term b is known as the constant term, and takes into acount inter-calibration errors between cells, inhomogeneities and energy absorbing material in front of the calorimeter. In a certain sense, b can be considered as the quality factor of a calorimeter, as constructional and mechanical errors reflect themselves in a larger constant term. The third term c is known as the noise term, and takes into account the electronic noise, pile-up and the radioactivity of the active and/or inactive medium. The stochastic and constant terms are often used to make comparisons between calorimeters.

The KLOE electromagnetic calorimeter, with design similar to that considered here, has a stated [3] energy resolution of

$$\frac{\sigma(E)}{E} = \frac{5.4\%}{\sqrt{E(\mathrm{GeV})}} + 0.7\%.$$

The constant term was said to be "negligible" in comparison to the stochastic term, and the dominant contribution to the resolution was sampling fluctuations, with a contribution from photoelectron statistics of 2.4%.

However, there is good reason to believe that the stated KLOE energy resolution is too optimistic. The Particle Data Book notes that "in almost all cases, installed calorimeters yield worse resolution than test beam prototypes" [4]. If we compare this result to the operational energy resolution

$$\frac{\sigma(E)}{E} = \frac{7.3\%}{\sqrt{E(\mathrm{GeV})}} + 3.6\%.$$

achieved by the RadPhi lead glass wall [5], we can not exclude the possibility that greater than usual care was given to gain matching, etc., in obtaining the KLOE result. A more

realistic energy resolution goal may be to assume a stochastic term similar to the KLOE result, and a constant term midway between the KLOE and RadPhi results:

$$\frac{\sigma(E)}{E} = \frac{5\%}{\sqrt{E(\mathrm{GeV})}} \oplus 2\%.$$

Like KLOE, the GlueX calorimeter has to deal with the issue of detector readout in the vicinity of a strong magnetic field. The light will either have to be piped to a lower magnetic field location, with a possibly large reduction in the amount of light collected and variations due to fiber couplings and fiber-to-fiber nonuniformities, or a new technology like SiPMs [6] will have to be used. These could cause the achieved resolution to be worse than the above goal, and so it is important to investigate how the BCAL invariant mass resolution depends upon the assumed energy resolution.

For this study, the stochastic term was varied between 3% and 7%, while the constant term was held fixed at 2.0%. In HDFast, the BCAL energy resolution is controlled via three MCFast parameters in the detector database file, `siga_em, sigb_em, sigc_em` [7], corresponding to the constants in the three above terms. The default resolution parameter values of $a = 6\%$, $b = 1\%$, are similar to those published by the KLOE Collaboration.

Position Resolution

Because of its cylindrical geometry, the BCAL position resolution must be parameterized differently in the longitudinal (z) and azimuthal (ϕ) directions.

The standard method [8] to determine the position of a particle that showers in a calorimeter is to reconstruct the center of gravity $(\bar{x}, \bar{y})$ of the energy E_i deposited in the various detector cells (with coordinates x_i, y_i) that contribute to the signal

$$\bar{x} = \frac{\sum_i x_i E_i}{\sum_i E_i}.$$

This resulting position resolution can be parameterized as

$$\sigma(x) = \frac{a}{\sqrt{E}} \oplus b.$$

The position resolution scales with $1/\sqrt{E}$ because the energy deposit E_i in cell i has a relative accuracy σ_i/E_i, which improves as $1/\sqrt{E_i}$, provided the shower profile stays the same. The resulting a can be from a few to as large as 20 mm, and b can be as small as

a fraction of a mm for a dense calorimeter with fine granularity. Typically, photon angular resolutions of about (45 mrad)/$\sqrt{E}$ are obtained, providing there is either depth-segmented readout, or a preshower counter [9]. For a detector at $R = 65$ cm, this corresponds to an effective position resolution of (2.9 cm)/$\sqrt{E}$.

This position resolution parameterization is applicable to any calorimeter which is pixelated in the plane transverse to the incident photons, such as the LGD, but the BCAL is planned to be a cylindrical fiber sandwich. In this case, the center of gravity method can only be used to determine the azimuthal position $\bar{\phi}$ of the showering particle. In his study [2], S. Teige assumed the BCAL position resolution was the same in all directions, parameterized as $\sigma = \frac{p}{\sqrt{E}}$, where p varied from 1 to 10 cm. A position resolution as large as 10 cm seems overly pessimistic, so for this study the ϕ-direction position resolution is varied between 1-5 cm/$\sqrt{E}$.

Like the KLOE calorimeter, the longitudinal component $\bar{z}$ of the hit particle direction will be obtained from the time difference $t_A - t_B$ of the signals from the two ends of the barrel. In this case, the z resolution depends upon the timing resolution of the BCAL readout system. The timing resolution of the KLOE electromagnetic calorimeter was measured using prompt photons from three different data samples: radiative $e^+e^- \to e^+e^-\gamma$, and the two radiative decays $\phi \to \eta\gamma \to 3\gamma$ and $\phi \to \pi^0\gamma \to 3\gamma$ [3]. They measured a time resolution of

$$\sigma(t) = \frac{56 \text{ ps}}{\sqrt{E(\text{GeV})}} \oplus 133 \text{ ps},$$

which yields a nearly constant $\sigma_t \approx 180$ ps for photon energies above 150 MeV, and a diverging time resolution for $E_\gamma < 75$ MeV. The first term is the sampling fluctuation term, and can be reduced by improving the calorimeter light collection. The constant term is mostly due to the intrinsic time spread due to the finite length in the z direction of the luminous point.

It seems reasonable to base the BCAL timing resolution goal upon the KLOE result

$$\sigma(t) = \frac{50 \text{ ps}}{\sqrt{E(\text{GeV})}} \oplus 150 \text{ ps}.$$

The initial timing performance of the SiPMs under consideration for the BCAL allow for the possibility that the obtained time resolution will be better than this. As the effective speed of light (including reflection) in the Kuraray scintillating fibers has been measured

[10] to be $v = 1.6 \times\ 10^8$ m/s, this corresponds to a z position resolution of

$$\sigma(z) = \frac{8 \text{ mm}}{\sqrt{E(\text{GeV})}} \oplus 24 \text{ mm}.$$

Note that this is comparable to the RadPhi LGD position resolution [5] of

$$\sigma(x) = \frac{7.1 \text{ mm}}{\sqrt{E(\text{GeV})}} \oplus X_0 \sin\theta$$

where X_0 is the radiation length of the glass. Thus, for this study the z-resolution sampling fluctuation term was held fixed at 0.8 cm, and the constant term was varied between 0.8 and 4.0 cm, corresponding to timing resolutions between 100 and 300 ps.

No position smearing is incorporated in the MCFast implementation of the BCAL detector, so in the HDFast package the BCAL position smearing is applied when root ntuples are generated from the root data trees (`.rdt` file). In its standard version, BCAL z position smearing is accomplished by the `-b` switch in `ntp_maker`, and has a default value of zero (no smearing). There is no ϕ smearing. For this study, `ntp_maker` was modified to provide smearing in both the z and ϕ directions, according to

$$\sigma(z) = \frac{z_{res}}{\sqrt{E}} \oplus 0.8\%, \quad \sigma(\phi) = \frac{\phi_{res}}{\sqrt{E}}.$$

The x and y track components were then smeared according to $\cos\phi$ and $\sin\phi$, where $\phi = p_y/p_x$.

III. SIMULATED REACTIONS

In selecting reactions for study, I considered only those which result in the reconstruction of a unique neutral particle. Reactions involving final states such as $\pi^0\pi^0 \to 4\gamma$, where it is necessary to determine which $\gamma\gamma$ pair correspond to each π^0, are complicated by combinatorics and so were not be considered. Five different reactions were chosen for study:

- $\gamma p \to pX^0 \to p\pi^+\pi^-\pi^0$. Reconstruct $\gamma\gamma \to \pi^0$.
- $\gamma p \to nX^+ \to n\omega^0\pi^+$, where $\omega^0 \to \pi^+\pi^-\pi^0$. Reconstruct $\gamma\gamma \to \pi^0$.
- $\gamma p \to pX^0 \to p\eta^0\pi^+\pi^-$, where $\eta^0 \to \gamma\gamma$. Reconstruct $\gamma\gamma \to \eta^0$.
- $\gamma p \to nX^+ \to n\eta^0\pi^+$, where $\eta^0 \to 3\pi^0 \to 6\gamma$. Reconstruct $6\gamma \to \eta^0$.
- $\gamma p \to nX^+ \to n\omega^0\pi^+$, where $\omega^0 \to \pi^0\gamma$. Reconstruct $3\gamma \to \omega^0$.

In all cases, X has a mass of 1.7 GeV and $\Gamma = 0.3$ GeV. The photon energy was fixed at 8 GeV.

The two η decay modes allow a comparison of the reconstruction resolution for the same meson into two channels with very different emitted photon energies. The $\omega \to \pi^0\gamma$ simulation is interesting in that it has many characteristics more similar to the η channels than to $\omega \to 3\pi$ decay. Some characteristics of the emitted photon distributions for all five reactions are listed in Table I. In the case of the two reactions with a single produced π^0, the largest proportion of the events are those with photons hitting the BCAL exclusively, while for the other three reactions, events in which γ hits are recorded in both the LGD and BCAL are the most common.

Several photon energy thresholds are also considered. These thresholds are applied to each cluster individually, and not to their sum. The results for a uniform 150 MeV threshold are presented to allow comparison to the report of S. Teige [2], where only events where all photons had energy greater than 150 MeV were used in the resolution calculations. In this case, showers from $\eta \to 2\gamma$ decay are almost all above the 150 MeV threshold, while very few from $\eta \to 3\pi^0$ survive. A more likely operational scenario for the GlueX experiment is to apply an energy threshold of 100-150 MeV to clusters detected by the LGD and to use a lower threshold of 20-30 MeV for clusters in the BCAL.

	$p\pi^0\pi^+\pi^-$	$n\omega^0\pi^+$ $(\omega \to \pi^0\pi^+\pi^-)$	$p\eta^0\pi^+\pi^-$ $(\eta \to 2\gamma)$	$n\eta^0\pi^+$ $(\eta \to 3\pi^0)$	$n\omega^0\pi^+$ $(\omega \to \pi^0\gamma)$
All complete events	93.0%	92.2%	93.6%	82.0%	91.0%
All complete events (150 MeV)	72.1%	62.1%	85.3%	27.2%	66.7%
All γs in BCAL	45.4%	38.2%	30.7%	14.8%	21.7%
All γs in BCAL (20 MeV)	44.2%	37.0%	30.4%	13.5%	21.0%
All γs in BCAL (150 MeV)	30.3%	19.4%	27.2%	1.4%	13.8%
All γs in LGD	25.2%	18.8%	11.1%	2.7%	6.7%
All γs in LGD (150 MeV)	24.6%	18.4%	11.1%	2.6%	6.6%
γs in BCAL and in LGD	22.4%	35.2%	51.8%	64.5%	62.6%
γs in BCAL and in LGD (150 MeV)	17.2%	24.3%	47.0%	23.2%	46.3%

TABLE I: Distribution of neutral decay products in the BCAL and LGD for the five simulated reactions, relative to all generated events. A 'complete' event has all γ and charged particles detected, while '150 MeV' has the requirement that each photon must deposit energy > 150 MeV. The middle two sections are the event fractions in which all γ are detected exclusively in the BCAL, or in the LGD, while in the bottom section γ hits were recorded for each event in both the BCAL and the LGD. Here, the LGD is taken to be a circular array of 1.16 m radius, with a 8×8 cm^2 beam hole, at z=5.75 m. The BCAL is assumed to be a cylinder of 0.67 m radius and 4 m length, with its upstream edge at z=0.17 m. The target center is at $z = 0.65$ m.

IV. RESULTS AND DISCUSSION

Only events where all photons exclusively intercept the BCAL, or all photons intercept only the LGD, were considered for further study. Mixed events, in which photon hits are recorded in both the LGD and BCAL, only complicate the invariant mass resolution study.

Energy Resolution

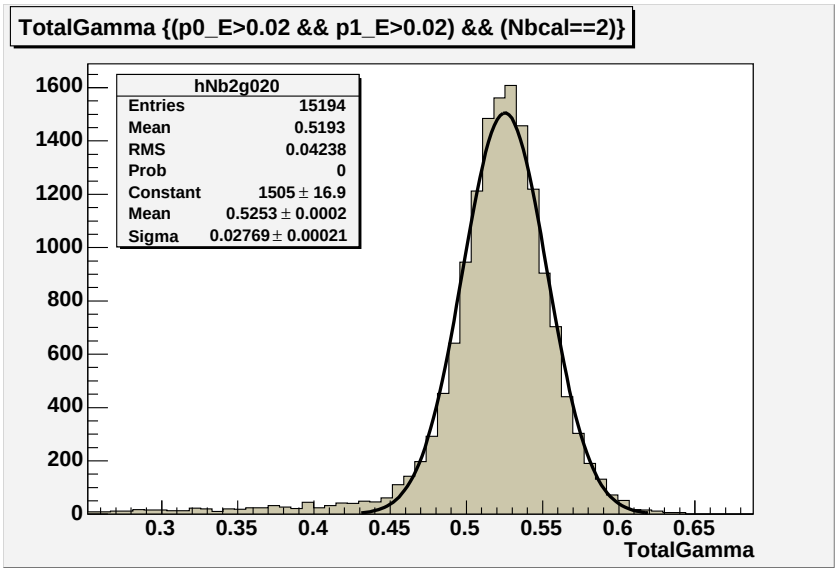

FIG. 1: $\gamma\gamma$ invariant mass distribution from the $\gamma p \rightarrow X^0 p \rightarrow p\eta^0\pi^+\pi^-$ reaction, for photons detected exclusively in the BCAL with a minimum of 20 MeV per shower. The simulation assumes a BCAL energy resolution of $5\%/\sqrt{E} \oplus 2\%$ and no position smearing.

Fig. 1 shows a representative BCAL $\eta^0 \rightarrow \gamma\gamma$ invariant mass distribution. In this case, the distribution exhibits a long low mass tail, so the RMS deviation from the mean is significantly larger than the σ of the fitted Gaussian distribution. While all BCAL simulations predict similar departures from purely Gaussian distributions, the low invariant mass tails are most pronounced in the $\eta^0 \rightarrow \gamma\gamma$ and $\omega^0 \rightarrow \pi^0\gamma$ simulations, in which case the tail comprises no more than 7% of the distribution. This tail is attributed to shower losses, as modeled by MCFast, which are not corrected for in the invariant mass reconstruction in HDFast. Because of the simplified treatment of the LGD in HDFast, showers detected exclusively in the LGD do not experience any losses, and do not exhibit any tail.

	BCAL RMS deviation	BCAL Gaussian σ	LGD RMS deviation
$p\pi^0\pi^+\pi^-$	20.7 MeV	17.1 MeV	7.1 MeV
$n(\omega \to \pi^0\pi^+\pi^-)\pi^+$	19.4 MeV	15.7 MeV	8.2 MeV
$p(\eta \to 2\gamma)\pi^+\pi^-$	85.5 MeV	31.1 MeV	23.2 MeV
$n(\eta \to 3\pi^0)\pi^+$	36.2 MeV	32.8 MeV	19.2 MeV
$n(\omega \to \pi^0\gamma)\pi^+$	89.8 MeV	38.9 MeV	30.3 MeV

TABLE II: Typical total gamma invariant mass resolutions obtained by the BCAL and LGD detectors for various reactions. For the BCAL, the resolution as measured two different ways is listed, the difference is due to the low mass tail in Fig. 1. For the LGD, the HDFast simulation gives a purely Gaussian peak, and so the two measures coincide. For the BCAL, the assumed energy smearing was $(5\%/\sqrt{E} \oplus 2\%)$, the assumed z-position smearing was $(2.4 \oplus 0.8/\sqrt{E})$ cm, and the assumed ϕ-position smearing was 3 cm$/\sqrt{E}$. For the LGD, the HDFast defaults of $(6\%/\sqrt{E} \oplus 2\%)$ energy smearing and no position smearing were used.

Table II lists some typical resolutions for both the BCAL and LGD. As expected, simulated invariant mass widths are somewhat larger when photons intercept the BCAL, compared to when they intercept the LGD. Since, in an experimental situation the low invariant mass tail will be eliminated by reconstruction corrections and analysis cuts, all further discussion will be based on the BCAL resolution obtained from the σ of the fitted Gaussian peak, rather than the RMS deviation from the mean. In this case, Table II indicates that the BCAL Gaussian σ depends more strongly upon the mass of the decaying neutral meson than upon the specific decay channel (i.e. σ is nearly the same for the two η^0 decay channels, and $\sigma_\pi < \sigma_\eta < \sigma_\omega$).

The dependence of the total photon invariant mass resolution upon the BCAL energy resolution is shown in Fig. 2. This result is somewhat sensitive to the shower energy deposition cut, particularly as it is increased to 150 MeV. In the case of the two η decay modes, the invariant mass resolutions degrade by a uniform 15 MeV as the energy resolution degrades from $(3\%/\sqrt{E} \oplus 2\%)$ to $(7\%/\sqrt{E} \oplus 2\%)$, independent of decay mode and energy cut. For neutral pions, the energy resolution degrades by about 7 MeV. The worst energy resolution is exhibited by $\omega^0 \to \pi^0\gamma$ decay, but it is still well below the invariant mass resolution requirement of $\sigma(m_{\Sigma\gamma}) < m_{\pi^0}/2$.

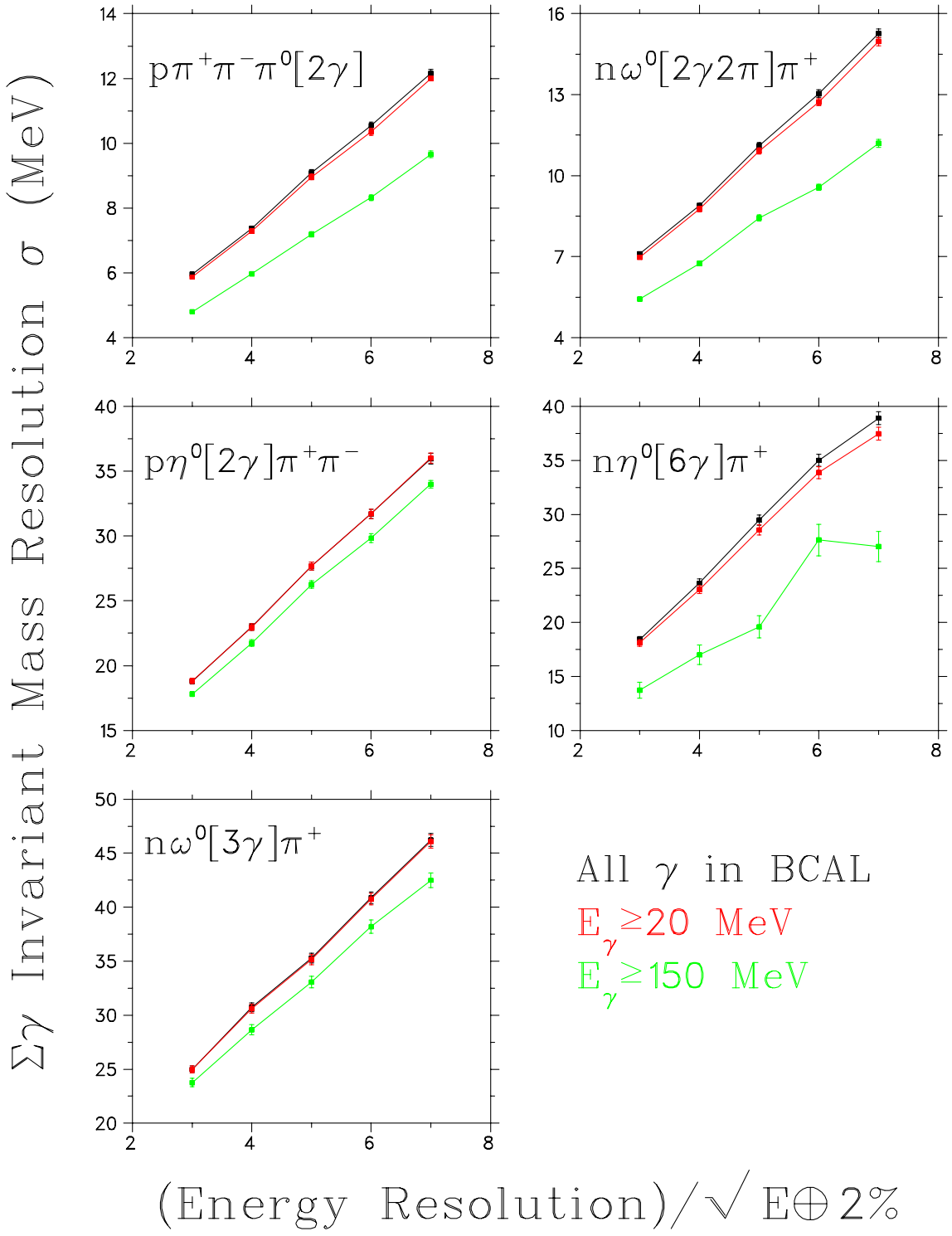

FIG. 2: Invariant mass resolution obtained for photons detected in the BCAL versus energy resolution. These curves incorporate no BCAL position smearing. The red and green curves have energy cuts applied to each detected cluster of 20 and 150 MeV, respectively, while the black curves are for all photons hitting the BCAL. The error bars indicate the statistical uncertainty in the simulations, and are largest for the $\eta \to 6\gamma$ simulation because of the small proportion of events passing the 150 MeV BCAL cut.

Position Resolution

The dependences of the simulated invariant mass resolution upon position smearing are shown for the five simulated reactions in Figs. 3-7. While the invariant mass resolutions depend only weakly upon z position resolution, they depend more strongly upon the assumed ϕ resolution. This is a geometric effect. Generally, the invariant mass σ degrades by 2-3 MeV as the z smearing is increased, but it degrades by 6-12 MeV as the ϕ smearing is increased, depending on the reaction and photon energy cut.

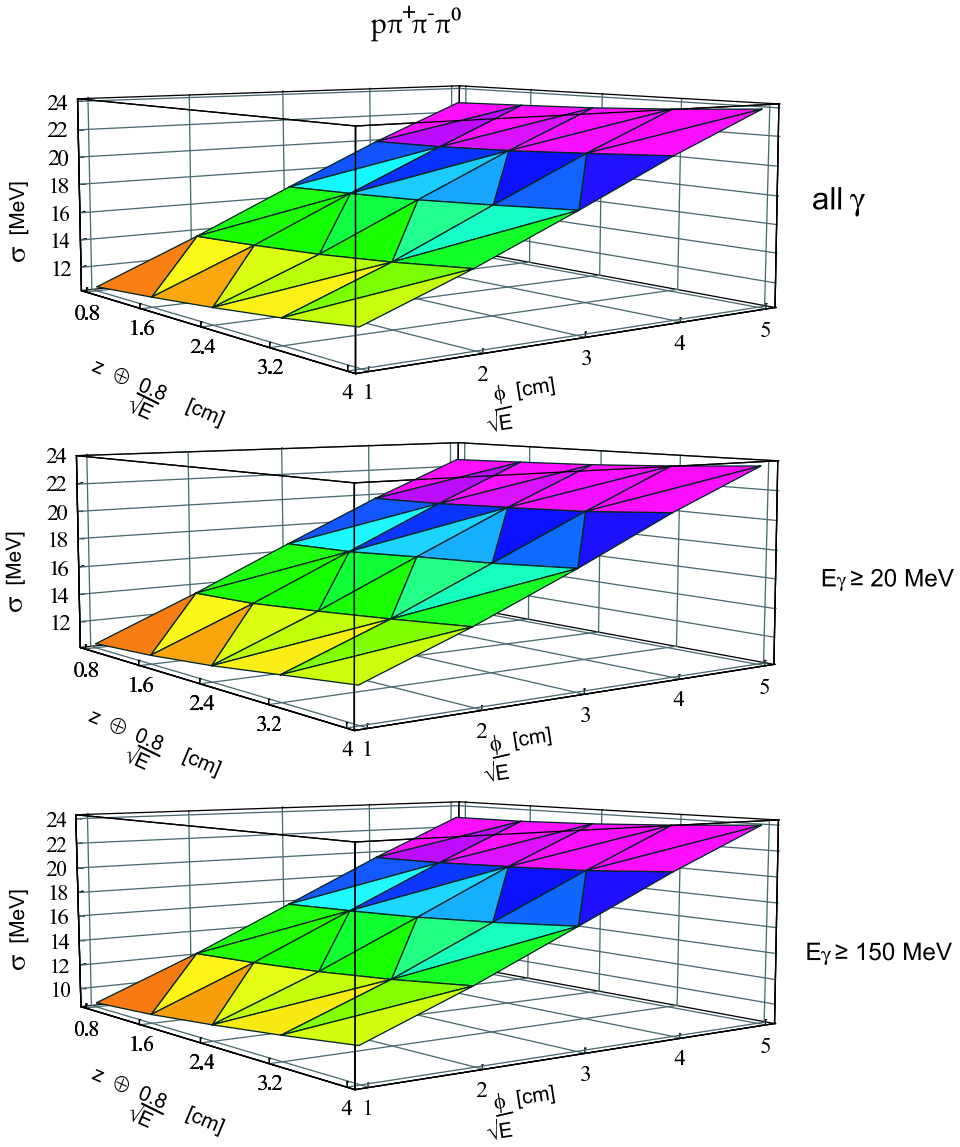

FIG. 3: π^0 invariant mass resolution from the $p\pi^0\pi^+\pi^-$ reaction for various simulated BCAL z and ϕ position resolutions. [3D plots courtesy of B. Leverington.]

For the two π^0 decay simulations (Figs. 3, 4), the invariant mass resolution degrades by about 10 MeV as the azimuthal position smearing is increased from (1 cm/$\sqrt{E}$) to (5 cm/$\sqrt{E}$). This is comparable to the 10 MeV increase displayed in the top two panels of Fig. 2 as the energy smearing is increased. For the two η^0 decay simulations (Figs. 5, 6), the dependence upon the ϕ position smearing is less, about 8 MeV over the range of simulated ϕ resolutions, compared to an energy resolution dependence of about 15 MeV in Fig. 2. The $\omega \to \pi^0\gamma$ invariant mass resolutions in Fig. 7 are the worst, but they are also the least sensitive to the position smearing.

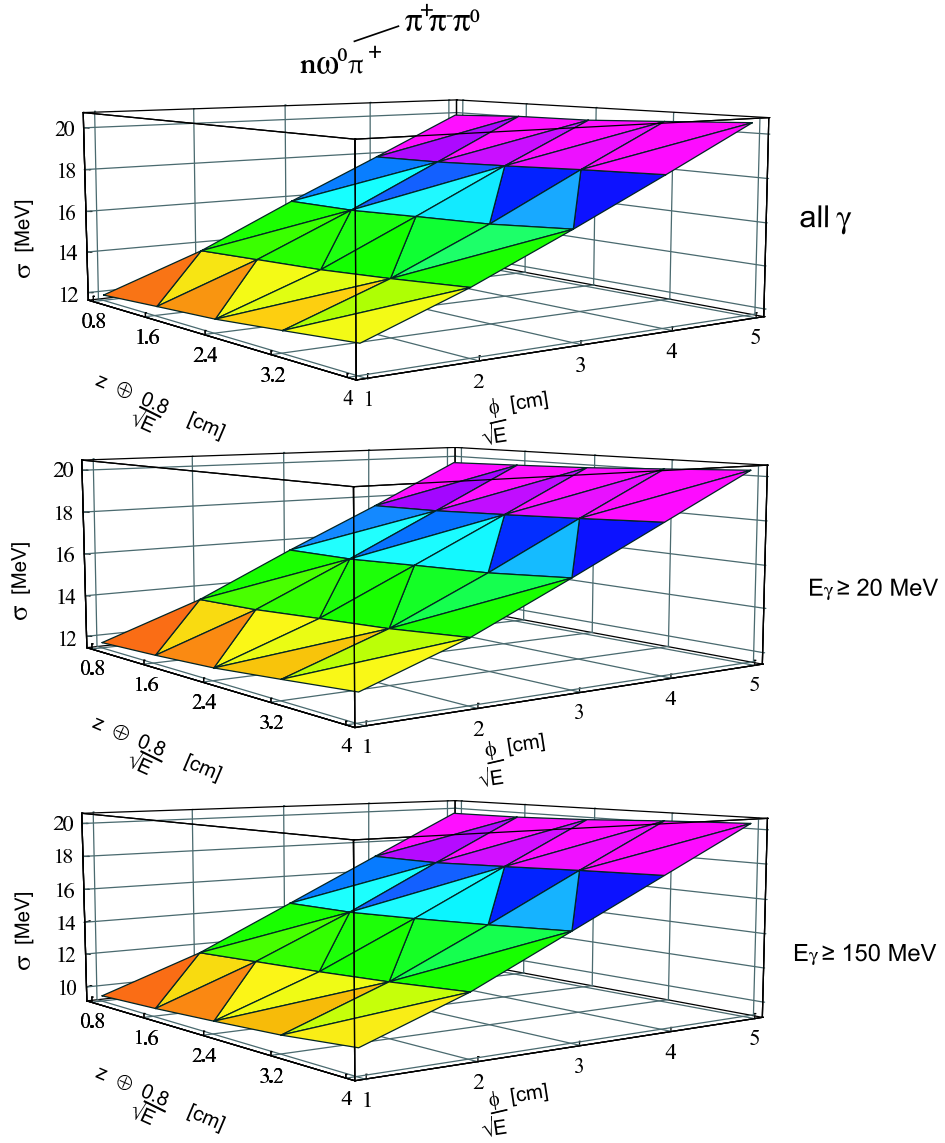

FIG. 4: π^0 invariant mass resolution from the $n(\omega \to \pi^0\pi^+\pi^-)\pi^+$ reaction for various simulated BCAL z and ϕ position resolutions. [3D plots courtesy of B. Leverington.]

The application of the photon energy cut improves the invariant mass resolution in all cases. This is most pronounced for the $6\gamma \rightarrow \eta^0$ simulation (Fig. 6), where the σ of the invariant mass distribution decreases by about 5 MeV as the photon energy cut is raised to 150 MeV, compared to a decrease of 1-2 MeV for the other simulations.

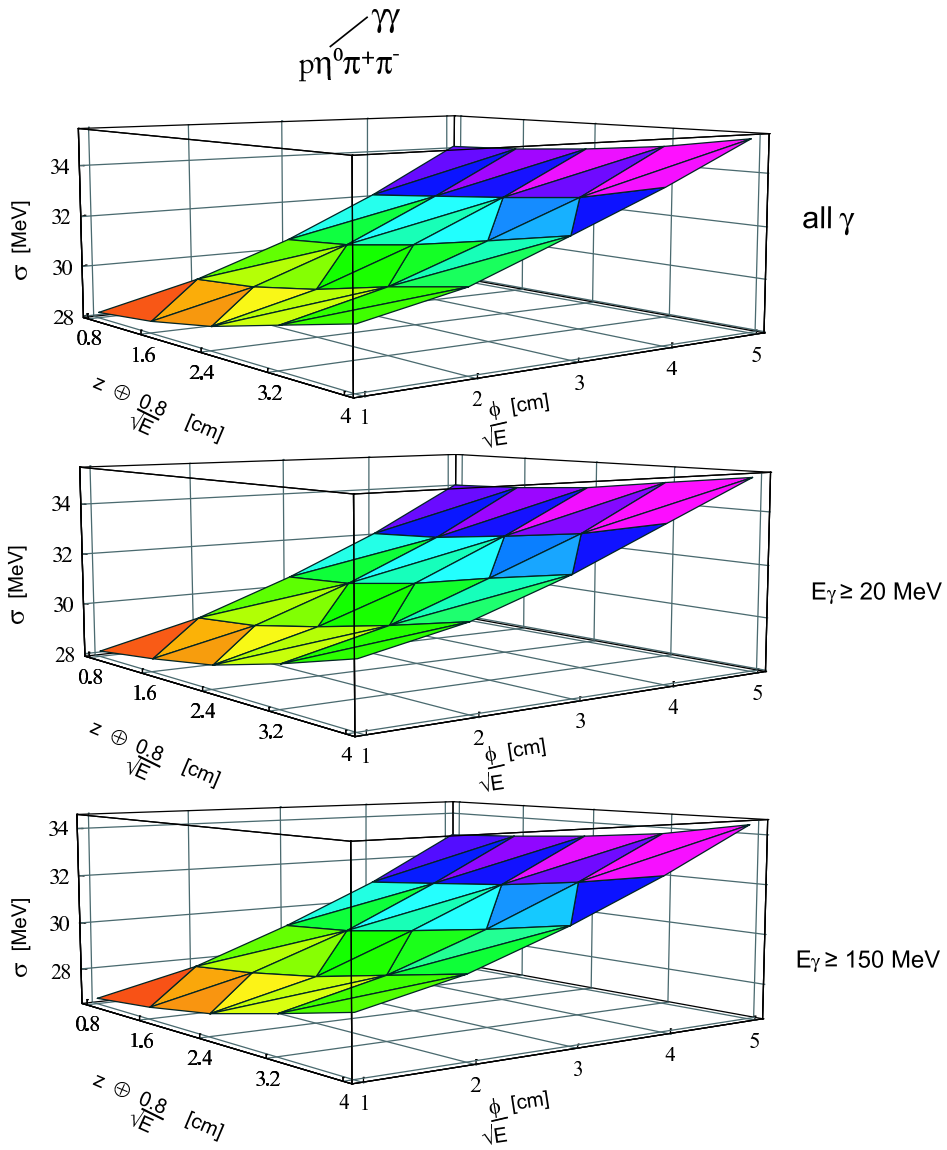

FIG. 5: η^0 invariant mass resolution from the $p(\eta \rightarrow \gamma\gamma)\pi^+\pi^-$ for various simulated BCAL z and ϕ position resolutions. [3D plots courtesy of B. Leverington.]

The $E_\gamma \geq 150$ MeV results in Figs. 2 and 5 can be compared directly to the 2001 BCAL resolution study by S. Teige [2]. Overall, the $\eta^0 \rightarrow \gamma\gamma$ mass resolutions obtained here are significantly better than those found in the earlier study, but the sensitivities to increases in the assumed position and energy resolutions are similar. Comparing to the 17-33 MeV

resolutions shown in the center left panel of Fig. 2, S. Teige's equivalent resolutions are 28-46 MeV. For constant $5\%/\sqrt{E}$ energy resolution, S. Teige finds the invariant mass resolution to increase from 36 to 48 MeV as the position resolution is increased from 1 cm/$\sqrt{E}$ to 5 cm/$\sqrt{E}$, compared to the 27-37 MeV found here. The lower resolutions found here are particularly baffling, given that S. Teige likely assumed a constant energy term of zero, as opposed to the 2.0% used here.

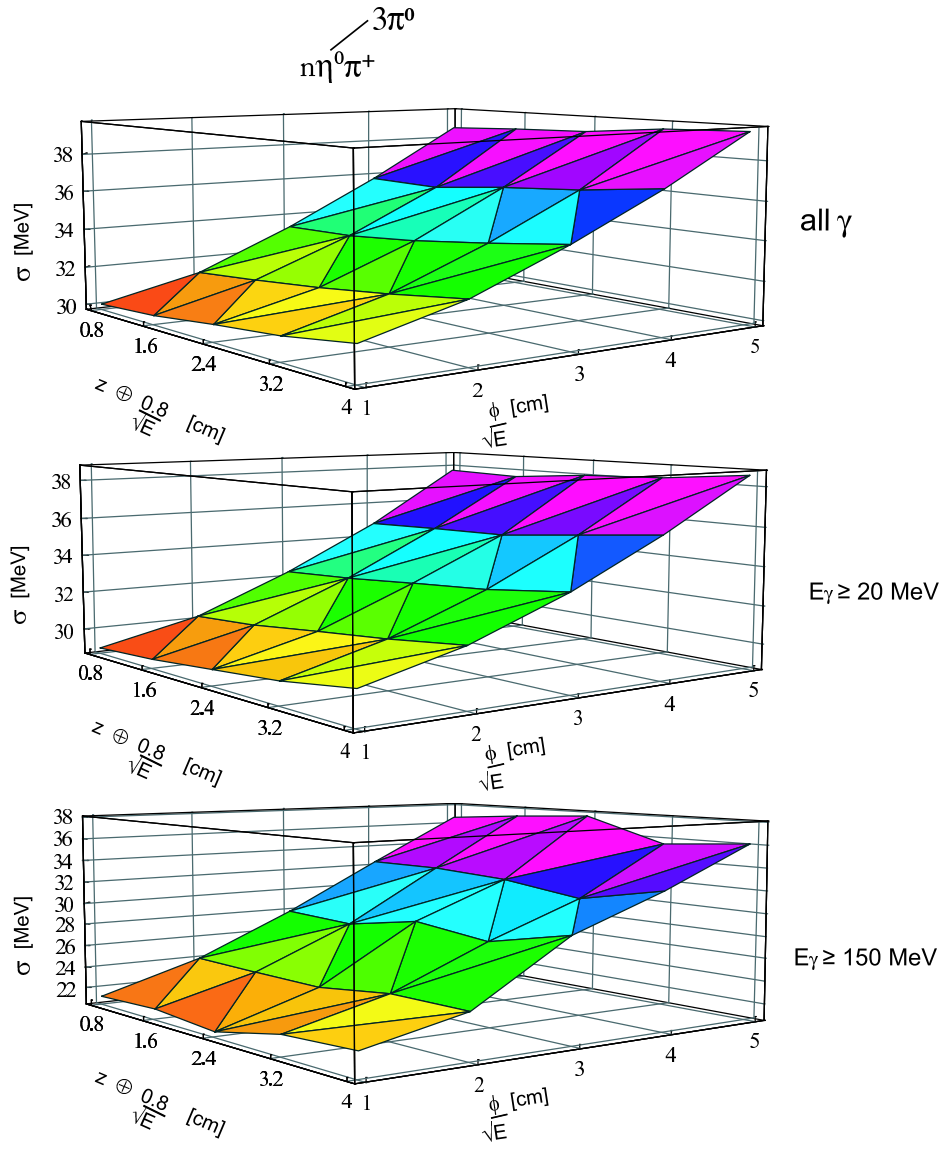

FIG. 6: η^0 invariant mass resolution from the $n(\eta \to 3\pi^0)\pi^+$ reaction for various simulated BCAL z and ϕ position resolutions. The anomalous resolution dependence in the bottom panel at large ϕres and $z$res is due to the limited statistics remaining after the $E_\gamma \geq 150$ MeV cut. [3D plots courtesy of B. Leverington.]

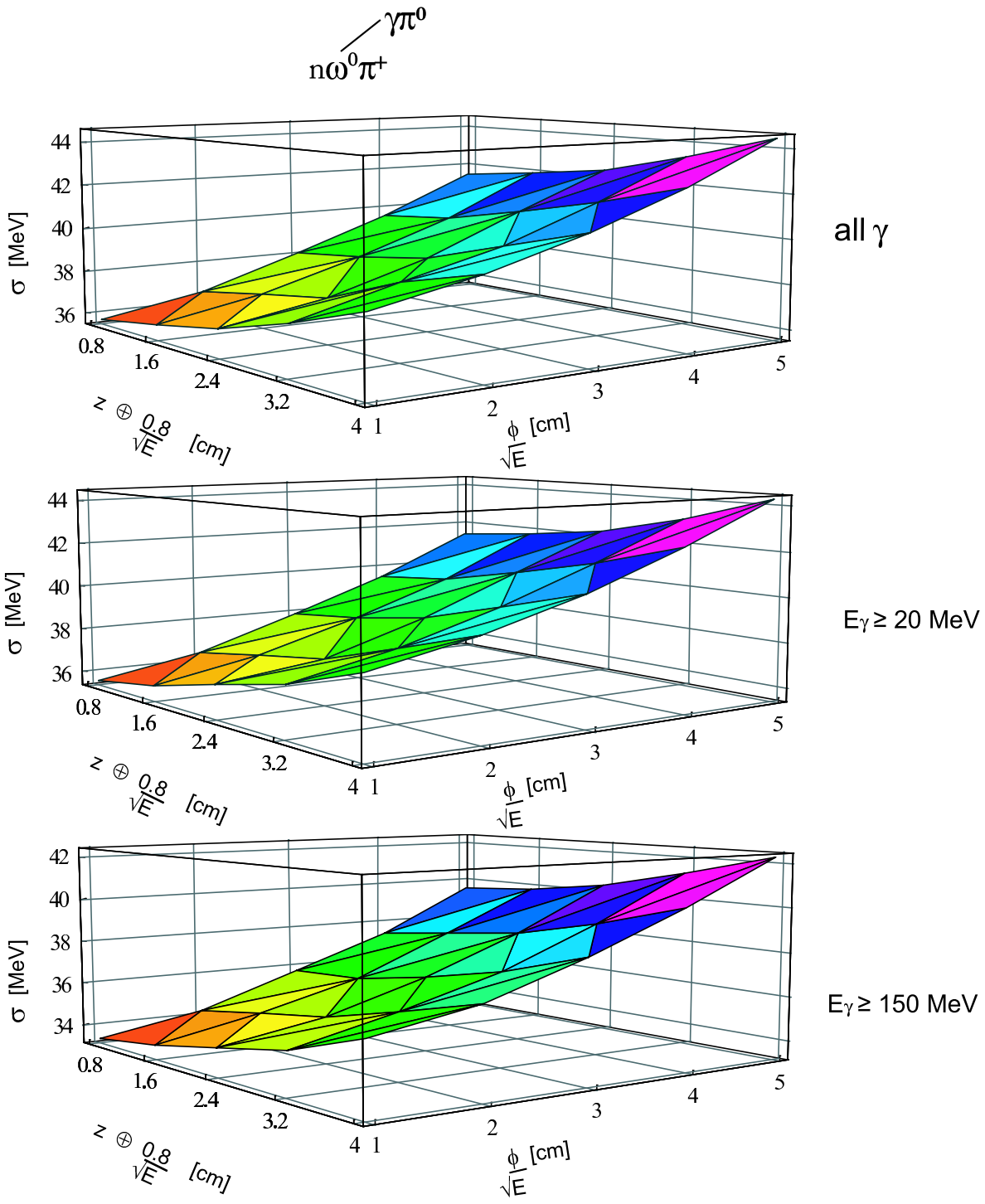

FIG. 7: ω^0 invariant mass resolution from the $n(\omega \to \pi^0\gamma)\pi^+$ reaction for various simulated BCAL z and ϕ position resolutions. [3D plots courtesy of B. Leverington.]

V. SUMMARY

The sensitivity of the BCAL invariant mass resolution to γ energy and position smearing has been studied using HDFast. Depending on the reaction observed, the simulated resolutions lie between 15 and 45 MeV, and in all cases is better than the minimum resolution requirement of $\sigma(m_{\Sigma\gamma}) < m_{\pi^0}/2$. The invariant mass resolution appears to be equally sensitive to reasonable variations in energy and position resolution from their expected values, but position resolutions in the z and ϕ directions do not contribute equally. Depending on the reaction, the invariant mass resolution is between 2 and 6 times more sensitive to the position resolution in the azimuthal (ϕ) direction than in the longitudinal (z) direction. This is a purely geometric effect due to the cylindrical layout of the detector. As the photon track enters the BCAL, its direction cosine in the z direction is large (grazing angle) but small in the ϕ direction (nearly perpendicular), giving a large relative magnification factor in the two directions. Optimizing the azimuthal position resolution might be an important consideration when deciding the azimuthal readout segmentation of the BCAL.

---

[1] GlueX/Hall D Design Resport, November, 2002.

[2] S. Teige, "BCAL Design Considerations", June 18, 2001.

[3] M. Adinolfi et al., Nucl. Instr. Meth. **A 494** (2002) 326-331.

[4] 2002 Particle Physics Data Booklet, p. 235.

[5] R. Jones, M. Kornicer, RadPhi LGD shower resolution study.

[6] V.D. Kovaltchouk, G.J. Lolos, Z. Papandreou, K. Wolbaum, "Comparison of a silicom photomultiplier to a traditional vacuum photomultiplier", Nucl. Instr. Meth., to appear, 2004.

[7] J. Yarba, "User's Guide for Showering/Calorimetry in MCFAST (version 4.1.0 and above)", November 10, 1999.

[8] M. Livan et al., "Scintillating-Fiber Calorimetry", CERN Yellow Report 95-02.

[9] 2004 Review of Particle Physics, Phys. Lett. B 592 (2004) Issues 1-4. Page 265.

[10] G.J. Lolos, Z. Papandreou, R. Filby, C. Ingram, B. Jasper, G. Koleva, B. Leverington, T. Summers, to be submitted to Nucl. Instr. Meth.